

Performance of 7T μ MRI-Based Virtual Bone Biopsy for Structural and Mechanical Analysis at the Distal Tibia

Y. A. Bhagat¹, C. S. Rajapakse¹, J. H. Love¹, M. J. Wald¹, J. F. Magland¹, A. C. Wright¹, H. K. Song¹, and F. W. Wehrli¹

¹Laboratory for Structural NMR Imaging, University of Pennsylvania, Philadelphia, PA, United States

INTRODUCTION: Advances in 3D micro-magnetic resonance imaging (μ MRI) allow direct visualization and quantification of trabecular bone (TB) architecture serially during senescence, disease progression and regression in response to treatment, and for fracture discrimination and prediction [1]. Additionally, finite element (FE) analysis applied to FE meshes generated from high resolution μ MRI can directly gauge the mechanical implications of structural changes [2]. Since the thickness of human skeleton trabeculae are on the order of 100-150 μ m, the detection of subtle microstructural TB alterations such as the conversion of plates to rods relies on adequate signal-to-noise ratio (SNR), which intrinsically governs the permissible spatial resolution and scan time. Currently, images of peripheral anatomical locations such as the distal tibia can be acquired in \sim 15 minutes with the in-plane resolution and slice thickness ranging from 137-190 μ m² and 160-410 μ m, respectively, at 1.5T and 3.0T [3]. With the emergence of ultra-high field (7.0T) whole body scanners, quantification of the TB microstructure is likely to benefit from the expected SNR gain, with one early report citing an SNR increase by a factor of 1.9 over 3.0T-based TB images [4]. Enhanced SNR should improve the detection sensitivity, particularly in longitudinal assessment of TB microstructural integrity potentially allowing earlier detection of structural changes following therapeutic interventions. Here, we have investigated the reproducibility of TB parameters derived from digital topological and FE analyses in a normal volunteer cohort using a new 3D fast spin echo (FSE) technique [5, 6] designed for TB structural imaging at 7.0T, operating within the specific absorption rate constraints at this field strength.

METHODS: The new pulse sequence [5, 6] has the following design features: A) a slab-selective excitation pulse, B) low RF-power depositing non-selective refocusing pulses, C) phase cycling to cancel undesired out-of-slab signal and D) high readout bandwidth to point spread function blurring. The chief objective of this work was to minimize scan-to-scan inconsistencies (coil positioning, motion degradation, registration) to maximize reproducibility and therefore discriminating power. The left distal tibiae of five normal male subjects (ages, 26-36 years) were scanned at 3 times (baseline, follow-up1 and follow-up 2) on a Siemens 7.0T whole body scanner (Erlangen, Germany) over a 3-month period. Due to the absence of an RF transmit body coil, a shielded Helmholtz pair transmit coil with a decoupled 4-element phased array receive coil (horseshoe geometry) operating at 297.2 MHz was used in a compact assembly to afford ankle and foot immobilization (Insight MRI, Worcester, MA) [7]. The 12-minute protocol consisted of 2D localizers and the 3D FSE with out-of-slab cancellation (OSC) sequence [5, 6] performed with: TR/TE= 500/20 ms, 8 echoes per TR, 4 shots, variable flip angle refocusing pulses (linearly decreasing from 180° to 90°), readout BW= 108 Hz/pixel, R>L phase encoding, 60% partial Fourier along k_x , FOV= 63x63x13 mm³ and a 460x460x32 data array yielding a resolution of 137x137x410 μ m³. GRAPPA (R=1.8, 30 ref. lines, 3x4 kernel) was also incorporated to further reduce the acquisition time to 10min 44s. In-plane translational motion correction was achieved by means of an autofocusing (AF) post-processing approach [8] targeted at optimizing an image quality metric, the L1-norm, against various trial phase shifts. Each image was manually masked to isolate the tibial TB region and full 3D transformations (3 rotations and 3 translations) were determined between baseline and follow-up images using a fast, rigid body registration algorithm [9]. Both follow-up images and their associated masks were then affine transformed (sinc-resampled by a factor of 3 in all three image coordinate axes) and the pre-determined rotations and translations were applied to induce alignment with the baseline reconstruction grid. Follow-up images were subsequently down-sampled to the original voxel size, followed by intersection with the baseline mask to facilitate comparison of parameters between the 3 exams. The masks were subjected to virtual bone biopsy processing [10] involving bone volume fraction (BVF (BV/TV)) mapping, skeletonization and digital topological analysis yielding surface-to-curve (S/C) ratio and erosion index (EI). FE analysis involved extraction of 5 x 5 x 5-mm³ cuboid subvolumes from the center of the TB region with image voxels converted to hexahedral finite elements [2]. Young's modulus and Poisson's ratio of pure bone tissue were chosen as 15 GPa and 0.3, respectively, and the Young's modulus of each finite element was set proportional to the BVF of the corresponding voxels. Finally, Young's moduli (E_{xx} , E_{yy} , E_{zz}) and shear moduli (G_{yz} , G_{zx} , G_{xy}) of the sub-volume were calculated using a FE solver developed in house by performing three compressive and three shear tests and solving for the compliance matrix. Coefficients of variation (CV) and intra-class correlation coefficients (ICC) served as metrics of reproducibility and reliability, respectively.

RESULTS AND DISCUSSION: Figure 1 provides a visual impression of the achieved reproducibility. Within-scan translational shifts of up to 7 pixels (\sim 900 μ m) were detected and corrected in 6/15 cases. The mean SNR over the 15 image acquisitions was 27.5 ± 2.05 , a 62% improvement over 3.0T derived FSE-OSC TB images with a 4-element receive coil of identical design [6]. Retrospective registration yielded an average common analysis volume of 67% across the 3 exams per subject. Scatterplots of select parameters highlight the discriminatory power of the technique despite the narrow age range of participating subjects (Figure 2). The reproducibility data for scale (BVF), topology (S/C and EI), elastic and shear moduli are given in Table 1. The ICC ranged from 0.95 to 0.99 for all parameters with the average CVs ranging from 2.4 to 4.9%, suggesting improved reproducibility compared to a similar study of distal radii at 1.5T (CVs of 2.4 to 9.3%) [11].

CONCLUSIONS: The results demonstrate that the new 7T imaging and analysis protocol provides highly reproducible measures of scale, topology and mechanical parameters of trabecular bone microstructure. The improved performance relative to prior MRI-based structure analysis is credited to enhanced SNR, improved subject motion control and correction, and superior retrospective registration techniques.

References: 1) Majumdar. *Top MRI* 13:323 (2002). 2) Rajapakse. *J Orthop Res* 27:1263 (2009). 3) Banerjee. *MRM* 21:818 (2005). 4) Krug. *MRM* 58:1294 (2007). 5) Magland. 17th ISMRM 1948 (2009). 6) Magland. *MRM* (in press). 7) Wright. 17th ISMRM 256 (2009). 8) Lin. *JMRI* 26:191 (2007). 9) Magland. *JMRI* 29:118 (2009). 10) Magland and Wehrli. *Acad Radiol* 15:1482 (2008). 11) Newitt. *Osteoporos Int.* 13:278 (2002). **Acknowledgements:** NIH RO1 AR53156, RO1 DK75648

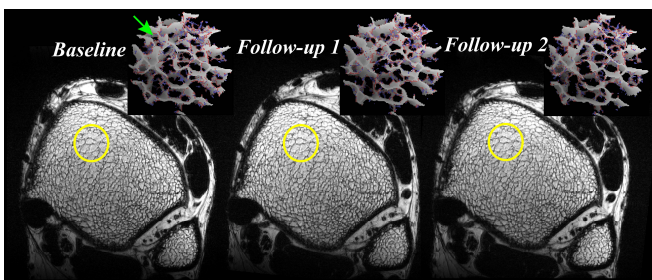


Figure 1: Representative axial FSE-OSC images of a healthy 36-year-old male subject across the 3 exams. 3D rendered skeletonized virtual cores ((69.5 μ m)³ voxels) visually illustrate similarity: surface voxels (gray), surface edges (red), curve voxels (blue) and small plate perforations (green arrow).

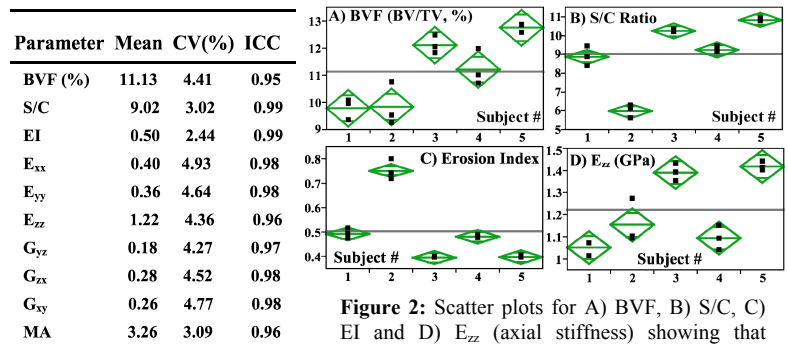


Figure 2: Scatter plots for A) BVF, B) S/C, C) EI and D) E_{zz} (axial stiffness) showing that means are significantly ($p < 0.001$) different for many pair-wise comparisons (One-way ANOVA).

Table 1: Means, CV and ICC for parameters relating scale, topology and elasticity (GPa) in 5 subjects. Mechanical Anisotropy, MA= $2E_{zz}/(E_{xx}+E_{yy})$

Parameter	Mean	CV(%)	ICC
BVF (%)	11.13	4.41	0.95
S/C	9.02	3.02	0.99
EI	0.50	2.44	0.99
E_{xx}	0.40	4.93	0.98
E_{yy}	0.36	4.64	0.98
E_{zz}	1.22	4.36	0.96
G_{yz}	0.18	4.27	0.97
G_{zx}	0.28	4.52	0.98
G_{xy}	0.26	4.77	0.98
MA	3.26	3.09	0.96